J|A|C|S ARTICLES

Published on Web 08/26/2009

Energetics of C−H Bond Activation of Fluorinated Aromatic Hydrocarbons Using a [Tp′Rh(CNneopentyl)] Complex

Meagan E. Evans,[†] Catherine L. Burke,[†] Sornanong Yaibuathes,[†] Eric Clot,[‡] Odile Eisenstein,[‡] and William D. Jones*,[†]

Department of Chemistry, University of Rochester, Rochester, New York 14627, and Institut Charles Gerhardt, Université Montpellier 2, CNRS 5253, case courrier 1501, Place E. Bataillon, 34095 Montpellier, France

Received June 19, 2009; E-mail: jones@chem.rochester.edu

Abstract: C−H bond activation of fluorinated aromatic hydrocarbons by [Tp′Rh(CNneopentyl)] resulted in the formation of products of the type Tp′Rh(CNneopentyl)($aryl_F$)H. The stability of the Rh−C_{aryl} product is shown to be strongly dependent on the number of ortho fluorines and only mildly dependent on the total number of fluorine substituents. Complexes with aryl groups containing two ortho fluorines have barriers to reductive elimination that are ∼5 kcal mol^{-1} higher than for those with a single ortho fluorine. Competition experiments along with $\Delta G_{re}^{\ddagger}$ values allow for the determination of relative Rh−C_{aryl} bond strengths and illustrate the large ortho fluorine effect on the strength of the Rh−C_{aryl} bond. A large change in Rh−C_{aryl} bond strength was measured for small changes in the respective calculated C−H bond strengths. Relating M−C to C−H bond strengths resulted in a line (slope = 2.14) that closely matches the theoretically calculated value (slope = 1.96). This is the first *experimental* quantization of an ortho fluorine effect as predicted by theory.

Introduction

The use of homogeneous transition-metal catalysts to activate and functionalize C−H bonds of hydrocarbons for industrial and synthetic purposes has been an active area of research.[1,2] While many organometallic complexes have been shown to activate C−H bonds, only a few have been useful in studying the kinetic and thermodynamic selectivity of C−H bond activation.[3−7] Understanding the selectivity of a metal fragment for different types of C−H bonds is vital for its use in synthetic transformations, and an improved knowledge of bond strengths lays the foundation for predicting selectivities.

Previously, Cp*Rh(PMe_3)H_2 and Tp′Rh(CNneopentyl)(η^2-PhN═C═N-neopentyl) complexes[3,10] (Cp* = C_5Me_5; Tp′ = tris(3,5-dimethylpyrazolyl)borate) have proven to be useful in studying kinetic selectivities due to their photochemical conversion to coordinatively unsaturated species that quickly react with C−H bonds of hydrocarbons. Both of these complexes show excellent solubility in a wide range of substrates such as aromatics, aliphatics, alkyl nitriles, alkyl chlorides, and fluoroarenes. It has been established that prior to aromatic C−H bond activation the metal center binds to the substrate through η^2-coordination of the arene double bond to the vacant sites on the metal.[11−14] A similar route is believed to be followed with aliphatic C−H bond activation going through a C−H σ-bond intermediate. However, this type of intermediate is less well documented,[15] but it has been observed in transient absorption experiments.[16−18]

Fluoroarenes offer the possibility for both C−H and C−F bond activation.[19−21] Calculations on osmium and rhodium complexes show that the barrier to oxidative addition of the C−F bond is ∼24 kcal mol^{-1} higher than that of C−H

[†] University of Rochester.
[‡] Université Montpellier 2.

(1) Parshall, G. W. *Science* **1980**, *208*, 1221.
(2) Nakao, Y.; Kashihara, N.; Kanyiva, K. S.; Hiyama, T. *J. Am. Chem. Soc.* **2008**, *130*, 16170.
(3) Vetter, A. J.; Rieth, R. D.; Jones, W. D. *Proc. Natl. Acad. Sci. U.S.A.* **2007**, *104*, 6957.
(4) Clot, E.; Eisenstein, O.; Jones, W. D. *Proc. Natl. Acad. Sci. U.S.A.* **2007**, *104*, 6939.
(5) Bryndza, H. E.; Fong, L. K.; Paciello, R. A.; Tam, W.; Bercaw, J. E. *J. Am. Chem. Soc.* **1987**, *109*, 1444.
(6) Bennett, J. L.; Wolczanski, P. T. *J. Am. Chem. Soc.* **1994**, *116*, 2179.
(7) Bennett, J. L.; Wolczanski, P. T. *J. Am. Chem. Soc.* **1997**, *119*, 10696.
(8) Selmeczy, A. D.; Jones, W. D.; Partridge, M. G.; Perutz, R. N. *Organometallics* **1994**, *13*, 522.
(9) Jones, W. D.; Hessell, E. T. *J. Am. Chem. Soc.* **1993**, *115*, 554.
(10) Jones, W. D.; Wick, D. D. *Organometallics* **1999**, *18*, 495.
(11) Jones, W. D.; Hessell, E. T. *J. Am. Chem. Soc.* **1992**, *114*, 6087.
(12) Belt, S. T.; Duckett, S. B.; Helliwell, M.; Perutz, R. N. *J. Chem. Soc., Chem. Commun.* **1989**, *14*, 928.
(13) Belt, S. T.; Dong, L.; Duckett, S. B.; Jones, W. D.; Partridge, M. G.; Perutz, R. N. *J. Chem. Soc., Chem. Commun.* **1991**, *4*, 266.
(14) Higgitt, C. L.; Klahn, A. H.; Moore, M. H.; Oelckers, B.; Partridge, M. G.; Perutz, R. N. *J. Chem. Soc., Dalton Trans.* **1997**, *8*, 1269.
(15) Vetter, A. J.; Flaschenriem, C.; Jones, W. D. *J. Am. Chem. Soc.* **2005**, *127*, 12315.
(16) Perutz, R. N.; Turner, J. J. *J. Am. Chem. Soc.* **1975**, *97*, 4791.
(17) Schultz, R. H.; Bengali, A. A.; Tauber, M. J.; Weiller, B. H.; Wasserman, E. P.; Kyle, K. R.; Moore, C. B.; Bergman, R. G. *J. Am. Chem. Soc.* **1994**, *116*, 7369.
(18) Bromberg, S. E.; Yang, H.; Asplund, M. C.; Lian, T.; McNamara, B. K.; Kotz, K. T.; Yeston, J. S.; Wilkens, M.; Frei, H.; Bergman, R. G. *Science* **1997**, *278*, 260.
(19) Edelbach, B. L.; Jones, W. D. *J. Am. Chem. Soc.* **1997**, *119*, 7734.
(20) Belt, S. T.; Helliwell, M.; Jones, W. D.; Partridge, M. G.; Perutz, R. N. *J. Am. Chem. Soc.* **1993**, *115*, 1429.
(21) Jones, W. D.; Partridge, M. G.; Perutz, R. N. *J. Chem. Soc., Chem. Commun.* **1991**, *4*, 264.

10.1021/ja905057w CCC: $40.75

addition.[22] While for some nickel and platinum complexes C−F activation seems to be preferred,[23−25] Perutz et al. found that [Cp*Re(CO)$_2$] was capable of activating C−H bonds of partially fluorinated aromatics.[26,27] Photolysis of the rhenium complex in pentafluorobenzene and tetrafluorobenzene led to C−H activation products only, while photolysis in *p*-difluorobenzene led to a mixture of the C−H activation product and the η^2-difluorobenzene complex in a 1:16 ratio. No C−H bond activation was observed for photolysis in benzene, and only the η^2-benzene complex was observed. Their study indicated that C−H activation of fluorinated aromatics was dependent on the stability of the η^2-arene precursor. Coordination to a double bond that contained a fluorine destabilized the benzene ring by inhibiting fluorine π-bonding, thus promoting C−H activation of the species.[28]

Jones and Perutz analyzed the kinetic and thermodynamic selectivity of [(C$_5$R$_5$)Rh(PMe$_3$)] (R = H, CH$_3$) with fluorinated aromatics and found that C−H activation products that maximize the number of ortho fluorines are thermodynamically favored.[8] This preference was attributed to an inductive effect of the ortho fluorine as shown earlier by Labinger and Bercaw, who examined metal−hydride and metal−alkyl bond strengths as a function of electronegativity differences.[29] C−H activation of *m*-difluorobenzene by the rhodium complex under thermodynamic conditions led to exclusive formation of the diortho fluorine complex, CpRh(PMe$_3$)(2,6-C$_6$F$_2$H$_3$)H. Formation of CpRh(PMe$_3$)(2,4-C$_6$F$_2$H$_3$)H and CpRh(PMe$_3$)(3,5-C$_6$F$_2$H$_3$)H was observed initially, but these were then easily converted to the thermodynamically preferred isomer.

Eisenstein and Perutz used calculations to predict an ortho fluorine effect on C−H activation products of fluorinated aromatic hydrocarbons by [CpRe(CO)$_2$].[30] A surprising result of their study was that the number of ortho fluorines strongly affected the M−C bond strength, while the *total* number of fluorines had only a minor effect on the M−C bond strength. All of the complexes with two ortho fluorines had calculated bond strengths ∼20 kJ mol^{-1} higher than those of complexes with one ortho fluorine. The slope of the plot of M−C vs H−C bond strengths also indicated a large ortho fluorine effect with a value of 2.25, much larger than the value for any previously examined metal−ligand system.[5−10] More recently, these authors reported the calculation of similar correlations for C−H activation of polyfluoroarenes for 13 different metal fragments (ZrCp$_2$ (Cp = η^5-C$_5$H$_5$), TaCp$_2$H, TaCp$_2$Cl, WCp$_2$, ReCp(CO)$_2$, ReCp(CO)(PH$_3$), ReCp(PH$_3$)$_2$, RhCp(PH$_3$), RhCp(CO), IrCp(PH$_3$), IrCp(CO), Ni(H$_2$PCH$_2$CH$_2$PH$_2$), and Pt(H$_2$PCH$_2$CH$_2$PH$_2$)). This report showed a similar correlation of the M−aryl bond strength with the C−H bond strength, with slopes ranging from 1.93 to 3.05. Furthermore, in all cases, the data points were clustered into groups with zero, one, or two ortho fluorines, as seen with [CpRe(CO)$_2$].[31]

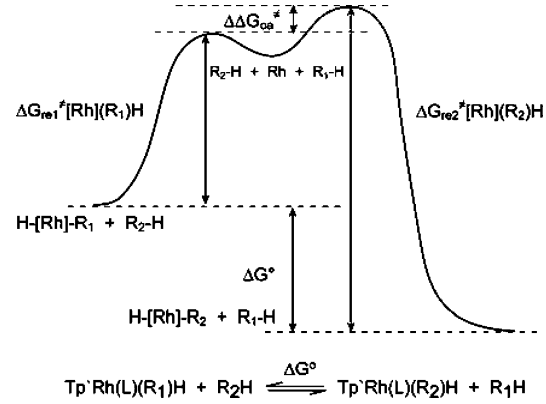

Figure 1. Free energy diagram for activation of hydrocarbon C−H bonds with [Tp′Rh(CNneopentyl)].

In previous work, Jones et al. examined the kinetic and thermodynamic selectivity of [Tp′Rh(CNneopentyl)] toward various hydrocarbon C−H bonds.[9,32] This 16-electron fragment forms as a result of photolysis of Tp′Rh(CNneopentyl)(η^2-PhN=C=N−R), which undergoes efficient photochemical loss of the carbodiimide ligand. Irradiation of this rhodium complex in neat hydrocarbon solvent results in rapid formation of the coordinatively unsaturated species, which then reacts quickly with the C−H bonds of alkanes and aromatics. The fast rate at which the rhodium inserts into the C−H bond of the hydrocarbon (∼200 ns)[33] indicates that the barrier to oxidative addition is small. This fragment also shows a preference for activation of the strong C−H bonds in aromatics over the weaker C−H bonds of aliphatics. Thermodynamic assessment of the C−H activation products indicates that this preference is due to the formation of stronger M−C bonds in arene C−H activation. Using the kinetic analysis shown in Figure 1, Jones and Hessell were able to measure the free energy of the reaction as indicated in eq 1.

$$\Delta G^\circ = \Delta G^{\ddagger}_{re2}([Rh](R_2)H) - \Delta\Delta G^{\ddagger}_{oa}(RH) - \Delta G^{\ddagger}_{re1}([Rh](R_1)H) \quad (1)$$

The kinetic selectivities ($\Delta\Delta G^{\ddagger}_{oa}$) were combined with the free energies of activation for reductive elimination of RH ($\Delta G^{\ddagger}_{re}$) to give the relative free energies (ΔG°) for the C−H activation complexes. Measurement of ΔG° along with known values for the C−H bond strengths allowed for the determination of relative M−C bond strengths, assuming that ΔG° and ΔH° parallel each other in these exchange reactions.[34] A plot of relative M−C bond strength [ΔD(M−C)] vs H−C bond strength [D(H−C)] resulted in a line with a slope of 1.2, indicating a 20% larger change in M−C bond strength for a given change in H−C bond strength. This type of plot allows for the prediction of unknown M−C bond strengths with known H−C bond strengths. Studies by Wolczanski using (^{t}Bu$_3$SiO)$_2$-

(22) Bosque, R.; Clot, E.; Fantacci, S.; Maseras, F.; Eisenstein, O.; Perutz, R. N.; Renkema, K. B.; Caulton, K. G. *J. Am. Chem. Soc.* **1998**, *120*, 12634.
(23) Reinhold, M.; McGrady, J. E.; Perutz, R. N. *J. Am. Chem. Soc.* **2004**, *126*, 5268.
(24) Schaub, T.; Fischer, P.; Steffen, A.; Braun, T.; Radius, U.; Mix, A. *J. Am. Chem. Soc.* **2008**, *130*, 9304.
(25) Cronin, L.; Higgitt, C. L.; Karch, R.; Perutz, R. N. *Organometallics* **1997**, *16*, 4920.
(26) Carbo, J. J.; Eisenstein, O.; Higgitt, C. L.; Klahn, A. H.; Maseras, F.; Oelckers, B.; Perutz, R. N. *J. Chem. Soc., Dalton Trans.* **2001**, 1452.
(27) Godoy, F.; Higgitt, C. L.; Klahn, A. H.; Oelckers, B.; Parsons, S.; Perutz, R. N. *J. Chem. Soc., Dalton Trans.* **1999**, *12*, 2039.
(28) Clot, E.; Oelckers, B.; Klahn, A. H.; Eisenstein, O.; Perutz, R. N. *Dalton Trans.* **2003**, 4065.
(29) Labinger, J. A.; Bercaw, J. E. *Organometallics* **1988**, *7*, 926.
(30) Clot, E.; Besora, M.; Maseras, F.; Mégret, C.; Eisenstein, O.; Oelckers, B.; Perutz, R. N. *Chem. Commun.* **2003**, 490.
(31) Clot, E.; Mégret, C.; Eisenstein, O.; Perutz, R. N. *J. Am. Chem. Soc.* **2009**, *131*, 7817.
(32) Wick, D. D.; Jones, W. D. *Organometallics* **1999**, *18*, 495.
(33) Lian, T.; Bromberg, S. E.; Yang, H.; Proulz, G.; Bergman, R. G.; Harris, C. B. *J. Am. Chem. Soc.* **1996**, *118*, 3897.
(34) This assumption amounts to assuming that the entropy changes associated with the exchange reactions are about the same.

(^{t}Bu$_3$SiNH)TiR on similar substrates showed a correlation of 1.36 for the plot of ΔD(M−C) vs D(H−C).[35] The experimental correlations found for the [Tp′Rh(CNneopentyl)] and (^{t}Bu$_3$SiO)$_2$-(^{t}Bu$_3$SiNH)TiR complexes have been reproduced by DFT calculations with good accuracy.[36] Earlier work by Bryndza and Bercaw demonstrated a 1:1 relationship between the strength of M−X and H−X for the metal fragments, Cp*Ru(PMe$_3$)$_2$(X) and (dppe)Pt(Me)(X),[37] where X encompassed many amines, alcohols, hydrides, alkyls, and cyanides.

Here we report the use of reductive elimination rates and kinetic selectivity experiments to measure the free energy for the reaction of [Tp′Rh(CNneopentyl)] with various fluoroarenes (eq 2). The free energy will be used in concert with calculated C−H bond strengths for fluorinated aromatics to ultimately determine relative M−C bond strengths for complexes of the type [Tp′Rh(CNneopentyl)(aryl$_F$)H]. A plot of ΔD(M−C) vs D(H−C) will be compared to computation results, and the magnitude of the ortho fluorine influence will be analyzed and quantified. The kinetic and thermodynamic selectivities will be compared to those previously reported by Jones and Perutz for C−H activation of fluorinated aromatics by both CpRe and CpRh complexes.

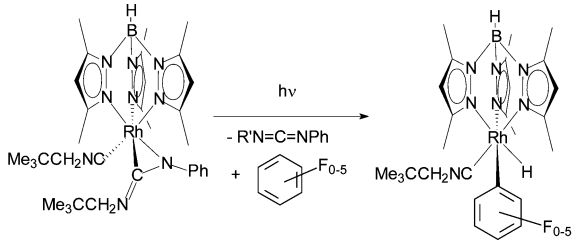

(2)

Results

Synthesis and Characterization. Tp′Rh(CNneopentyl)(η^2-Ph-N═C═N-neopentyl) (**1**) was dissolved in neat fluoroarene and irradiated for 30 min at low temperature, resulting in the formation of products of the type Tp′Rh(CNneopentyl)(aryl$_F$)H (see Scheme 1). Irradiation products were analyzed by ^{1}H and ^{19}F NMR spectroscopy, as described below (see Supporting Information for all spectra).

Photolysis of **1** in pentafluorobenzene results in bleaching of the bright yellow solution. Removal of the solvent, followed by ^{1}H NMR analysis of the residue in benzene-d_6, shows the clean formation of Tp′Rh(CNneopentyl)(C$_6$F$_5$)H (**2**). The ^{1}H NMR spectrum of complex **2** displays a triplet resonance at δ −13.17 for the metal hydride. The complex is chiral at rhodium, resulting in six resonances between δ 1.1 and 2.4 for the six Tp′ methyl groups and three resonances between δ 5.4 and 5.8 for the three Tp′ methine hydrogens (Supporting Information, Table S-1). The ^{1}H{^{19}F} NMR spectrum (Figure 2) for complex **2** reduces the triplet hydride resonance to a doublet, verifying that the hydride is coupled to only one fluorine (and rhodium) with J = 17 Hz. The ^{19}F NMR spectrum displayed five distinct fluorine signals between δ −43.5 and −103.6, with the two ortho fluorines being farthest downfield and the two meta fluorines being farthest upfield as was the case for other rhodium−fluoroaryl complexes.[8] The presence of five fluorine resonances indicates that there is hindered rotation of the fluoroarene around the Rh−C$_{aryl}$ bond. ^{19}F NMR spectra were collected at elevated temperatures as high as 100 °C, yet no evidence for rotation was observed.

Scheme 1. Products of Photolysis of **1** in Various Fluorinated Aromatic Hydrocarbons

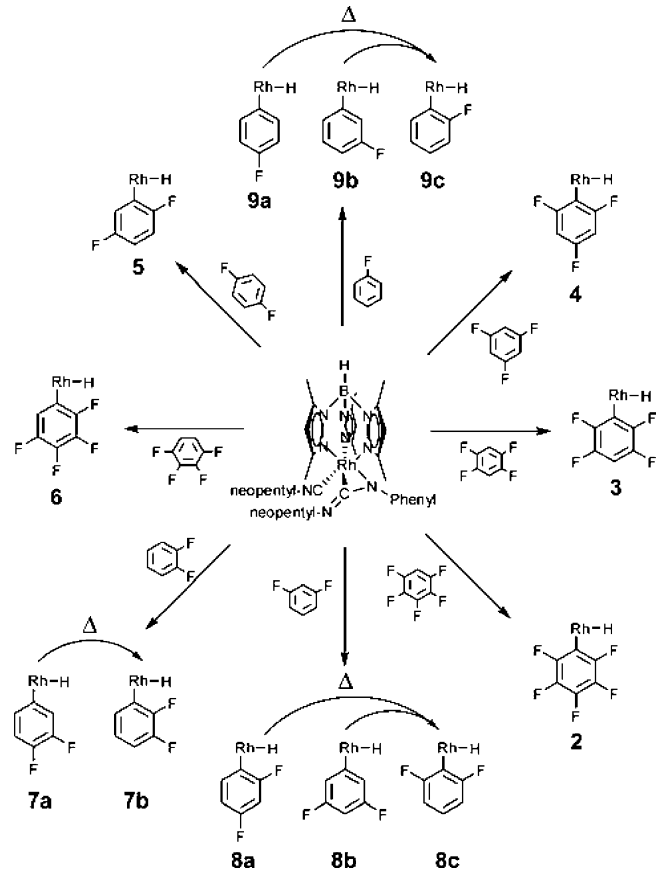

Treatment of **2** with CCl_4 resulted in the formation of Tp′Rh(CNneopentyl)(C$_6$F$_5$)Cl (**2-Cl**), which was characterized by X-ray diffraction (Figure 3). The ^{19}F NMR spectrum of **2-Cl** shows five fluorine signals between δ −47.47 and −101.95, again indicative of hindered aryl−Rh rotation (see Supporting Information). The structure shows that the aryl group interdigitates with the pyrazolylborate groups, such that the plane of the aryl group contains the three-fold Rh−B axis. In this geometry, one of the ortho fluorine atoms is in close proximity to the chlorine, suggesting that it is the fluorine in this position that couples to the hydride in **2**. The non-fluorinated parent molecule, Tp′Rh(CNneopentyl)(C$_6$H$_5$)H, shows hindered rotation at room temperature (broad aryl resonances) but can be

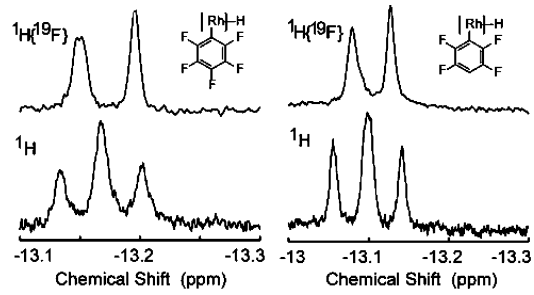

Figure 2. ^{1}H and ^{1}H{^{19}F} NMR spectra (400 MHz) of the hydride resonances for complexes **2** and **3** showing direct coupling of the hydride to one of two ortho fluorines.

(35) Bennett, J. L.; Wolczanski, P. T. *J. Am. Chem. Soc.* **1997**, *119*, 10696.
(36) Clot, E.; Mégret, C.; Eisenstein, O.; Perutz, R. N. *J. Am. Chem. Soc.* **2006**, *128*, 8350.
(37) Bryndza, H. E.; Fong, L. K.; Paciello, R. A.; Tam, W.; Bercaw, J. E. *J. Am. Chem. Soc.* **1987**, *109*, 1444.

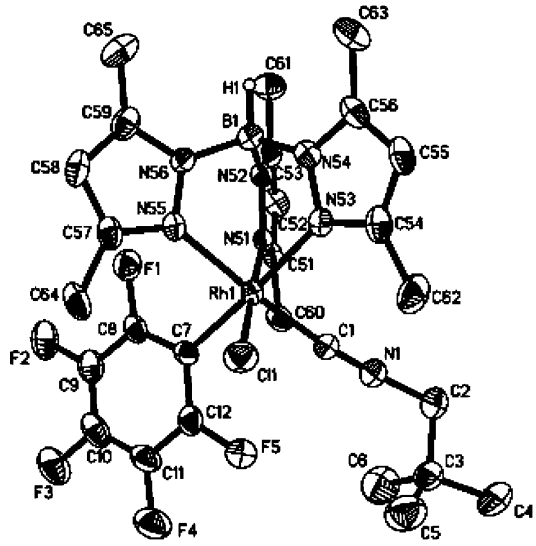

Figure 3. ORTEP drawing of Tp′Rh(CNneopentyl)(C_6F_5)Cl (**2-Cl**). Hydrogen atoms except on boron have been have been omitted for clarity.

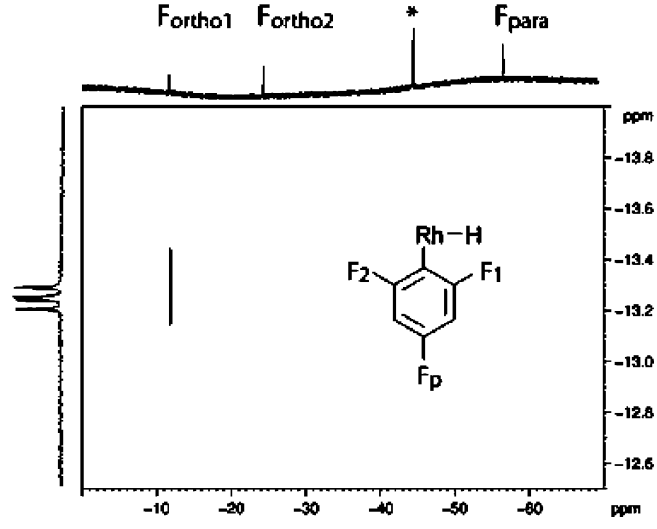

Figure 4. $^1H-^{19}F$ HETCOR NMR spectra (400 MHz) of **4** showing that one ortho fluorine is coupled to the hydride. ^1H (hydride region) and ^{19}F NMR spectra for **4** are plotted along the *y*- and *x*-axes, respectively. * indicates free $C_6H_3F_3$.

frozen out at low temperature.[38] Table S-2 (Supporting Information) contains selected X-ray collection data.

Photolysis of **1** in 1,2,4,5-tetrafluorobenzene results in clean formation of Tp′Rh(CNneopentyl)(2,3,5,6-C_6F_4H)H (**3**), which also displays a metal hydride resonance at δ −13.09 as a triplet. The $^1H\{^{19}F\}$ NMR spectrum again reduced the hydride to a doublet, showing that the hydride splitting is due to coupling from both rhodium and one fluorine (Figure 2). The ^{19}F NMR spectrum shows hindered rotation of the fluoroarene as four fluorine resonances are observed between δ −44.78 and −80.12. The two ortho fluorines appear downfield, while the two meta fluorines appear upfield.

Photolysis of **1** in 1,3,5-trifluorobenzene results in the clean formation of Tp′Rh(CNneopentyl)(2,4,6-$C_6F_3H_2$) (**4**), showing a single metal hydride resonance at δ −13.23 in the ^1H NMR spectrum that is resolved as a doublet of doublets due to rhodium and fluorine coupling (Figure 4). Three unique resonances were observed in the ^{19}F NMR spectrum between δ −11.83 and −57.11, indicating hindered rotation of the fluoroaryl group. A 2D $^1H-^{19}F$ HETCOR experiment (Figure 4) further demonstrated that only one downfield fluorine is coupled to the hydride.

Photolysis of **1** in *p*-difluorobenzene resulted in the formation of Tp′Rh(CNneopentyl)(2,5-$C_6F_2H_3$)H (**5**), with a metal hydride resonance at δ −13.38 appearing as a well-resolved doublet of doublets (see Supporting Information). The ^{19}F NMR spectrum showed two fluorine resonances at δ −29.35 and −60.44 for the ortho and meta fluorines. Complex **5** is distinct from **2**−**4** in that two distinct rotamers might have been expected due to hindered rotation around the Rh−aryl bond. However, only one rotamer is observed in the ^1H and ^{19}F NMR spectra. Free rotation of the fluoroarene can be discounted, as the J_{F-H} value is similar to those observed previously in **2**−**4**. Were the fluoroaryl group rotating freely, the averaged J_{F-H} value would be expected to be about half the value in the former complexes. In addition, ^{19}F NMR spectra collected at low temperatures (−80°) still showed only one rotamer. ^1H NMR spectra collected at elevated temperatures (up to 80 °C) did not show any changes either. The photolysis in *p*-difluorobenzene also resulted in formation

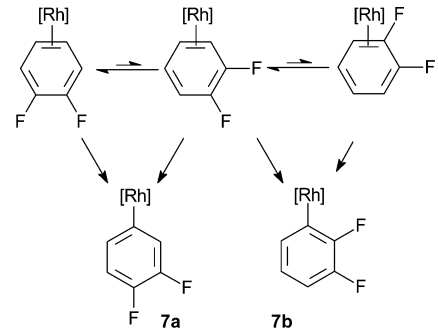

Figure 5. Photolysis of **1** in *o*-difluorobenzene gives products **7a** and **7b** in a ratio of 1.5:1. The major product is a result of rhodium binding to the fluoroarene at the less sterically hindered positions.

of small amounts of the *o*-, *m*-, and *p*-C−H activation products of the released carbodiimide ligand (∼5%),[39] indicating that difluorobenzene does not compete with the liberated carbodiimide as well as the tri-, tetra-, and pentafluorobenzenes.

Similar observations were made using 1,2,3,4-tetrafluorobenzene to produce Tp′Rh(CNneopentyl)(2,3,4,5-C_6F_4H)H (**6**). As in the previous case, only one of two possible rotamers was observed, with a hydride resonance at δ −13.40 appearing as a doublet of doublets. The ^{19}F NMR spectrum showed four unique fluorine signals between δ −48.88 and −103.24.

Irradiation of **1** in *o*-difluorobenzene resulted in the formation of two products, Tp′Rh(CNneopentyl)(3,4-$C_6F_2H_3$)H (**7a**) and Tp′Rh(CNneopentyl)(2,3,-$C_6F_2H_3$)H (**7b**), in a ratio of 1.5:1. Complex **7a** is thought to be more favored kinetically, as there is a greater abundance of less sterically hindered (and hence more favored) η^2-complexes that can lead to its formation (Figure 5). It has previously been shown that prior to C−H bond activation the rhodium binds to the arene through the π-system of the double bond.[40] The ^1H NMR spectrum for **7a** displays a broad hydride doublet at δ −13.76 (J_{Rh-H} = 23.5 Hz) due to hindered Rh−aryl rotation at room temperature.[11] No fluorine

(38) Hessell, E. T.; Jones, W. D. *Organometallics* **1992**, *11*, 1496.

(39) Vetter, A. J.; Rieth, R. D.; Brennessel, W. W.; Jones, W. D. *J. Am. Chem. Soc.* **2009**, *131*, 10742.

(40) Jones, W. D.; Feher, F. J. *J. Am. Chem. Soc.* **1986**, *108*, 4814.

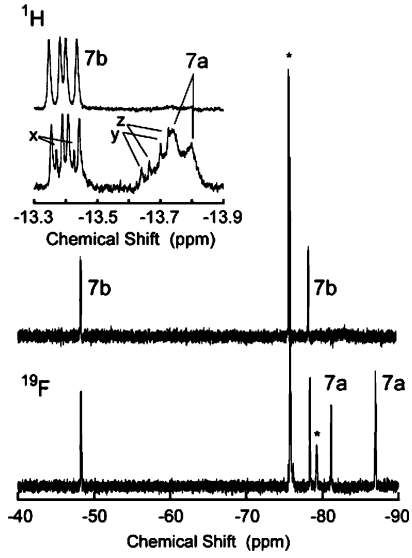

Figure 6. ^{1}H NMR spectra of hydride resonance and ^{19}F NMR spectra for products **7a** and **7b**. The bottom ^{1}H and ^{19}F NMR spectra show the kinetic products formed after photolysis at −20 °C. The top ^{1}H and ^{19}F NMR spectra show the thermodynamic product that remains after warming the product mixture at 100 °C for 10 days. * indicates residual solvent resonances.

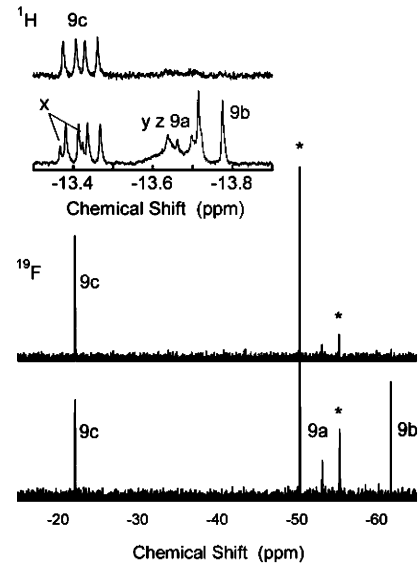

Figure 7. ^{1}H NMR of hydride region and ^{19}F NMR for products **9a**, **9b**, and **9c**. The bottom ^{1}H and ^{19}F NMR spectra show the kinetic products formed after photolysis. The top ^{1}H and ^{19}F NMR spectra show the thermodynamic product that remains after warming the product mixture at 100 °C for 10 days. * indicates residual solvent resonances.

coupling was observed. The hydride resonance for **7b** appeared as a doublet of doublets at δ −13.39, with both Rh−H and F−H couplings. Four fluorine resonances were observed in the ^{19}F NMR spectrum between δ −48.26 and −86.96, with the ortho fluorine of **7b** being the most downfield. The ^{1}H NMR spectrum also showed the presence of three C−H activation products at δ −13.39, −13.66, and −13.68 corresponding to meta (**x**), ortho (**y**), and para (**z**) C−H bond activation of the phenyl ring of the released carbodiimide ligand. Upon heating this initial product mixture consisting of **7a**, **7b**, **x**, **y**, and **z** to 100 °C for 10 days in neat *o*-difluorobenzene, **7a** converts to **7b** and **x**, **y**, and **z** disappear. The ^{1}H and ^{19}F NMR spectra show only the presence of **7b** (Figure 6).

Photolysis of **1** in *m*-difluorobenzene resulted in the formation of three C−H activation products, Tp′Rh(CNneopentyl)(2,4-$C_6F_2H_3$)H (**8a**), Tp′Rh(CNneopentyl)(3,5-$C_6F_2H_3$)H (**8b**), and Tp′Rh(CNneopentyl)(2,6-$C_6F_2H_3$)H (**8c**), in a ratio of 10:4:1. The ^{1}H NMR spectrum displayed three hydride resonances at δ −13.49, −13.63, and −13.15. The hydride resonances for **8a** and **8c** appeared as doublets of doublets due to both fluorine and rhodium coupling, while the hydride resonance for **8b** appeared as a simple doublet due to rhodium coupling only. The ^{19}F NMR spectrum showed six fluorine signals between δ −19.62 and −54.23, with the three ortho fluorines being the farthest downfield. The major product was identified as **8a** on the basis of the ^{19}F NMR spectrum, which showed the presence of one downfield ortho fluorine and one para fluorine. Complex **8b** was identified by the presence of two upfield meta fluorine resonances, and complex **8c** was identified by the presence of two small downfield ortho fluorine resonances. The ^{1}H NMR spectrum also showed the presence of three C−H activation products corresponding to carbodiimide C−H activation (**x**, **y**, and **z**). This kinetic product mixture consisting of **8a**, **8b**, **8c**, **x**, **y**, and **z** was heated to 100 °C for 12 days in neat *m*-difluorobenzene, resulting in the disappearance of **x**, **y**, and **z**. The ratio of **8a**:**8b**:**8c** was now 1.2:0.5:1, showing that **8a** and **8b** were slowly converting to **8c**, although decomposition slowly set in as the sample continued to be heated.

Photolysis of **1** in fluorobenzene resulted in the formation of three C−H activation products, Tp′Rh(CNneopentyl)(4-C_6H_4F)H (**9a**), Tp′Rh(CNneopentyl)(3-C_6H_4F)H (**9b**), and Tp′Rh(C-Nneopentyl)(2-C_6H_4F)H (**9c**), in a ratio of 1:2:2. The ^{1}H NMR spectrum displayed three hydride resonances between δ −13.42 and −13.74 for ortho, meta, and para C−H activation of the fluoroarene, along with a small amount of three hydride resonances for products **x**, **y**, and **z**. The hydride resonances for complexes **9a** and **9b** appear as doublets, while the hydride resonance for **9c** displays a doublet of doublets pattern due to the additional ortho fluorine coupling. The hydride resonance for complex **9a** could not be clearly resolved, as it is broadened due to hindered aryl rotation and it overlaps with the ortho and para C−H activation product resonances of **y** and **z**. The ^{1}H NMR spectra showed ∼18 resonances for the Tp′ methyl groups, but only the Tp′ methyl groups on **9c** were readily identified. This kinetic product mixture consisting of **9a**, **9b**, **9c**, **x**, **y**, and **z** was heated to 100 °C for 10 days in neat fluorobenzene, resulting in the disappearance of **x**, **y**, and **z** and the conversion of **9a** and **9b** to **9c**. The ^{1}H and ^{19}F NMR spectra of the resulting solution show only the presence of **9c** (Figure 7).

Reductive Elimination of Fluoroarenes. The rates for reductive elimination of complexes **2**−**6**, **7b**, and **9c** were determined by monitoring the conversion of the complexes to Tp′Rh-(CNneopentyl)(C_6D_5)D (**10-**d_6) by ^{1}H NMR spectroscopy (eq 3). These experiments were performed at 138.5 °C, and in each

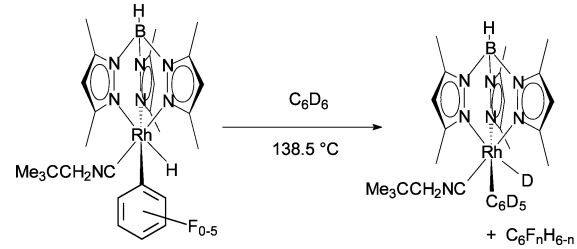

(3)

case formation of **10-**d_6 was irreversible. For complexes **2**, **4**, **5**, **7b**, and **9c**, a plot of ln([C]$_t$/[C]$_0$) of the fluoroarene activation

Table 1. Rates of Reductive Elimination of RH from Tp′Rh(CNneopentyl)(R)H at 138.5 °C

R	k_{re}(RH), s^{-1}	$\Delta G^{\ddagger}_{re}$, kcal mol^{-1}
pentafluorophenyl, **2**	$2.46(4) \times 10^{-7}$	36.81(1)
2,3,5,6-tetrafluorophenyl, **3**	$4.64(9) \times 10^{-7}$	36.29(1)
2,4,6-trifluorophenyl, **4**	$5.07(3) \times 10^{-7}$	36.22(4)
2,5-difluorophenyl, **5**	$3.63(7) \times 10^{-5}$	32.72(1)
2,3,4,5-tetrafluorophenyl, **6**	$1.76(8) \times 10^{-6}$	35.20(3)
2,3-difluorophenyl, **7b**	$5.97(7) \times 10^{-5}$	32.32(9)
2-fluorophenyl, **9c**	$3.53(7) \times 10^{-4}$	30.86(1)
phenyl[a]	$7.8(2) \times 10^{-3}$	28.33(3)

[a] Calculated at 138.5 °C from activation parameters in ref 7. Errors are reported as standard deviations.

Table 2. Kinetic Selectivity Data Determined from Competition Experiments[a]

entry	substrates	T (°C)	k_1/k_2	$\Delta\Delta G^{\ddagger}_{oa}$[b]
1	1,2,4,5-tetrafluorobenzene: pentafluorobenzene	10	0.723	–0.18
2	1,3,5-trifluorobenzene: pentafluorobenzene	10	1.92	+0.37
3	*p*-difluorobenzene: pentafluorobenzene	–20	3.93	+0.69
4	1,2,3,4-tetrafluorobenzene: pentafluorobenzene	–20	3.18	+0.58
5	benzene:pentafluorobenzene	10	30.2	+1.92

[a] All samples were irradiated for 30 min with 0.2 mL of each substrate used, except for entry 5 which used 0.05 mL of benzene and 0.4 mL of pentafluorobenzene. [b] A positive value indicates that C_6F_5H is kinetically disfavored.

complex vs time was used to determine the rates of reductive elimination. For complexes **3** and **6**, the reactions showed a first-order decay to equilibrium, so these rates were determined by a fitting program (see Experimental Section). Table 1 summarizes the rate constants k_{re}(RH) along with the activation energies for the reductive elimination at 138.5 °C ($\Delta G^{\ddagger}_{re}$).

The reductive elimination of fluoroarene from complexes **2**−**4** occurred with the slowest rates, ranging from 2.4×10^{-7} to 5.0×10^{-7} s^{-1}. Complete elimination of fluoroarene was observed for complexes **2** and **4**, while complex **3** went to ∼85% completion. These results showed that the presence of two ortho fluorine atoms greatly stabilizes the Rh−C bond. Complexes **5**, **6**, **7b**, and **9c** each contain one ortho fluorine atom and had rates for reductive elimination of fluoroarene much faster than those of the diortho fluorine complexes, ranging from 3.5×10^{-4} to 1.7×10^{-6} s^{-1}. Each of these eliminations went to completion except for that of tetrafluoroaryl product **6**, which went to ∼80−85% completion. The mono-ortho fluorine complexes have rates of reductive elimination of fluoroarene that are much faster than those of the diortho species, but they are still much slower than the rate of reductive elimination of benzene from the unsubstituted phenyl hydride complex. It is interesting to note that complex **6** (with four total fluorine atoms) has a reductive elimination rate that is faster than that of complex **4** (with three total fluorine atoms). However, **4** has two ortho fluorines, while **6** only has one. The stability of the Rh−C bond is strongly dependent on the number of ortho fluorines as opposed to the total number of fluorine atoms.

Competition Experiments. The rate at which two substrates compete for the vacant sites in [Tp′Rh(CNneopentyl)] was determined by irradiation of **1** in a known ratio of two solvents and monitoring the kinetic products formed by ^{1}H NMR spectroscopy (see Table 2). Only substrates that resulted in the formation of one product were used in this study. Consequently, fluorobenzene, *o*-difluorobenzene, and *m*-difluorobenzene were not used in the competition experiments. The selectivities k_1/k_2 reported in Table 2 were calculated on a per-molecule basis using eq 4,

$$\frac{k_1}{k_2} = \left(\frac{I_1}{I_2}\right)\left(\frac{V_2}{V_1}\right)\left(\frac{d_2}{d_1}\right)\left(\frac{MW_1}{MW_2}\right) \quad (4)$$

where I_1/I_2 is the integration area, V_2/V_1 is the ratio of solvent volumes, d_2/d_1 is the solvent density ratio, and MW_1/MW_2 is the ratio of solvent molecular weights; subscript 2 refers to C_6F_5H and subscript 1 refers to the competing fluoroaryl substrate. The mild selectivities resulted in small differences in $\Delta\Delta G^{\ddagger}_{oa}$ values (∼1 kcal mol^{-1}).

Discussion

The activation of C−H bonds in fluoroaromatics comes as no surprise, considering the preference seen for C−H activation with both [Cp*Rh(PMe_3)] and [CpRh(PMe_3)]. This is in contrast to an electron-rich fragment such as [Ni(dippe)], which shows a preference for C−F activation in fluoroarenes. In the case of [Tp′Rh(CNR)], only C−H activation of the aromatic bonds is observed. When the fluoroarene possesses more than one type of C−H bond, all possible regioisomers are observed. Some arenes proved less reactive than others, and in these cases reaction of the aromatic C−H bonds of the liberated carbodiimide was competitive.

In every case where multiple regioisomers were observed, the kinetic products converted to a single thermodynamically preferred product. For example, fluorobenzene showed initial formation of all three regioisomers, which upon heating to 100 °C showed complete conversion to the *o*-fluoro isomer. Likewise, 1,2-difluorobenzene gave two regioisomers, which convert to a single *o*-fluoro isomer upon heating. The only case that was a bit unusual was that of 1,3-difluorobenzene. Initially, the three anticipated isomers were observed to form, but upon heating, conversion to the most stable 2,6-difluoroaryl product (with two ortho fluorines) was observed to occur only slowly, contrary to what was seen with the Cp*Rh and CpRh analogues. This lack of reactivity cannot be attributed to crowding in the Tp′Rh system, since 1,3,5-trifluorobenzene and pentafluorobenzene have no problem forming a C−H activation product with two ortho fluorines. Consequently, the lack of rearrangement is attributed to the lower reactivity of a difluoro-substituted arene vs a more highly fluoro-substituted arene.

Tp′Rh(CNR)PhH was observed to show hindered rotation, as evidenced by the presence of broad resonances for the phenyl group in the ^{1}H NMR spectrum at room temperature. Upon cooling to −40 °C, the resonances sharpened to produce five distinct signals for the aromatic protons. Similarly, fluoroaryl complexes also show evidence for hindered rotation at room temperature. For example, complexes with two ortho fluorines (**2**−**4**) showed that all fluorines on the aromatic ring were distinct in the ^{19}F NMR spectrum, even at elevated temperatures. Complexes with only one ortho fluorine (**5**, **6**, **7b**, **8a**, and **9c**) also showed evidence of only one of two possible rotamers. Apparently, the orientation of the plane of the phenyl ring between the two pyrazolyl rings renders the orientation with the ortho fluorine away from the Tp′ ligand as the preferred rotamer. Even complexes with no ortho fluorines show evidence for hindered rotation. Complex **8b** shows two distinct fluorine resonances for the two meta fluorine atoms ($\Delta\nu$ = 814 Hz). The aromatic resonances in the ^{1}H NMR spectrum are broad, also consistent with hindered rotation.

Table 3. Kinetic and Thermodynamic Data for Formation of Tp′Rh(CNneopentyl)(R)H (All Values in kcal mol^{-1})

R	$\Delta\Delta G^{\ddagger}_{oa}$[a]	ΔG°[a]	calcd D(R−H)[b]	exptl D(Rh−C)$_{rel}$[c]	calcd D(Rh−C)$_{rel}$[c]
pentafluorophenyl	0	0	123.0	13.5	13.25
2,4,6-trifluorophenyl	+0.37	0.23	123.2	12.9	10.86
2,3,5,6-tetrafluorophenyl	−0.18	0.70	122.5	11.9	12.49
2,3,4,5-tetrafluorophenyl	+0.58	1.03	120.6	9.6	9.11
2,5-difluorophenyl	+0.69	3.40	119.8	6.2	7.06
phenyl	+1.92	6.56	117.1	0.0	0.00

[a] Relative to pentafluorobenzene. [b] From ref 31. [c] Relative to benzene. ΔH corrected for number of hydrogens available for activation.

The rates of reductive elimination of complexes **2**−**6**, **7b**, and **9c** were all measured at 138.5 °C. This temperature was chosen as **2** was slow to eliminate C_6F_5H (τ = 32 d), yet the rate of elimination of C_6H_5F from **9c** could still be measured (τ = 33 min). The rate constants were seen to be proportional to the number of ortho fluorines on the phenyl ligand. The greater stability of aryl complexes with ortho fluorines has been noted in a number of other systems and is generally referred to as the "ortho fluorine effect". For the range of rates observed, the free energy barriers for reductive elimination were found to span the range 28−37 kcal mol^{-1}.

In complexes where more than one isomer of C−H activation product could form, the kinetic products are consistent with the initial formation of intermediate η^2-arene complexes in which the lack of fluorine substituents on the double bond bound to the metal is kinetically preferred. These η^2-arene complexes then activate one of the C−H bonds on the double bond bound to the metal. By the reverse of this process, the metal can competitively migrate around the arene ring to eventually arrive at a double bond where C−H activation produces a Rh−phenyl product containing an ortho fluorine bond. This complex is thermodynamically preferred, and further isomerization is prevented. It is interesting to note that, for *m*-difluorobenzene, formation of **8a** and **8b** is seen initially (along with a trace of **8c**), and **8b** converts into **8a** with one ortho fluorine, but further conversion to **8c** is slow and decomposition occurs. Consequently, in this case, the lack of additional fluorines appears to decrease the binding ability of the η^2-arene complex.

Thermodynamic Assessment. As mentioned earlier, the results from the reductive elimination and kinetic selectivity experiments can be used together to determine the thermodynamics for fluoroarene C−H bond activation. The relative free energy values (ΔG°) for complexes **2**−**6** were determined by subtracting the $\Delta\Delta G^{\ddagger}_{oa}$(RH) and $\Delta G^{\ddagger}_{re}$(RH) values from the $\Delta G^{\ddagger}_{re}$ for pentafluorophenyl complex **2** (eq 5), as indicated in Scheme 1, where $R_2H = C_6F_5H$ and $R_1H = C_6F_nH_{6-n}$ (Table 3).

$$\Delta G^{\circ} = \Delta G^{\ddagger}_{re}(\mathbf{2}) - \Delta\Delta G^{\ddagger}_{oa} - \Delta G^{\ddagger}_{re}(Ar^FH) \qquad (5)$$

Using these measured ΔG° values along with known (calculated) C−H bond strengths of fluorobenzenes, the relative Rh−C bond strengths of the C−H activation complexes can be determined using eq 6,

$$\begin{aligned} D_{rel}(Rh{-}C) &= [\Delta H(Rh{-}R_2) - \Delta H(Rh{-}R_1)] \\ &= \Delta G^{\circ} + RT\ln(H_1/H_2) + [\Delta H(R_2{-}H) - \\ &\quad \Delta H(R_1{-}H)] \end{aligned} \qquad (6)$$

which includes the assumption that $\Delta\Delta G^{\circ} \approx \Delta\Delta H^{\circ} - RT\ln(H_1/H_2)$, where H_1/H_2 is the ratio of the number of hydrogens on the substrates; i.e., the ΔS° values are the same for these reactions,[9] other than the statistical contribution for the number of hydrogens. These Rh−C bond strengths are *relative* to the Rh−C bond strength in the benzene C−H activation product, which is set to 0 kcal mol^{-1}. As can be seen in Table 3, the pentafluorobenzene activation complex was determined to have the strongest Rh−C bond, at 13.5 kcal mol^{-1} greater than that of the benzene activation complex. Both the 2,3,5,6-tetrafluorophenyl and 2,4,6-trifluorophenyl activation complexes had similar bond strengths, at 11.9 and 12.9 kcal mol^{-1} higher, respectively, than that of the benzene activation complex. The 2,3,4,5-tetrafluorophenyl and 2,5-difluorophenyl activation complexes were determined to have bond strengths significantly lower than those of the other fluoroaryls, at 9.6 and 6.2 kcal mol^{-1}, respectively, relative to that of the benzene activation complex.

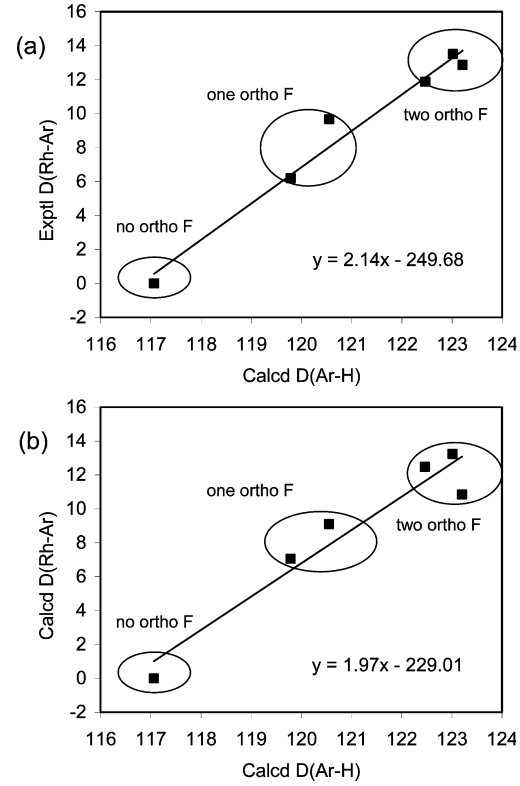

Figure 8. Plot of relative Rh−C_{aryl} bond strength vs calculated C−H bond strength (kcal mol^{-1}). (a) Experimentally determined D(Rh−C_{aryl}) and (b) DFT-calculated D(Rh−C_{aryl}).

A plot of calculated C−H bond strengths[28] vs the experimentally determined relative Rh−C bond strengths shows a good linear correlation with a slope of 2.14 (Figure 8a), indicating that the effect of fluorine is greater on the strength of the M−C bond than on the strength of the C−H bond. For comparison with the experimental values for this system, DFT calculations were performed on the corresponding fluoroaryl compounds using the model fragment [HB(pyrazolyl)$_3$Rh(CNMe)] (see Supporting Information). These calculated Rh−C_{aryl} bond strengths are also listed in Table 3. A plot of calculated C−H bond strengths[28] vs calculated relative Rh−C bond strengths shows a good linear correlation, with a slope of 2.0 (Figure 8b). The resemblance with the experimentally determined values is uncanny.

Finally, it is worth commenting on the origin of the "ortho fluorine effect". As noted in the earlier work by Perutz, Eisenstein, and Clot, there is a strong correlation between the

slope of these plots and the ionic character in the metal−aryl bond.[30,31] As the contribution of ionic character to the bond increases, it is expected that M−C bond strengths will increase significantly more than C−H bond strengths, as metals are more polarizable than hydrogen. The effects observed (and calculated) here are entirely in line with this interpretation.

Conclusions

Photolysis of Tp′Rh(CNneopentyl)(η^2-Ph-N═C═N-neopentyl) in neat fluoroarenes resulted in C−H activation products of the type Tp′Rh(CNneopentyl)(aryl$_F$)H in high yield. The kinetic selectivities were directed by the sterics of the η^2-arene species, while thermodynamic selectivities displayed a strong preference for C−H activation ortho to the maximum number of fluorines. Complexes with two ortho fluorines had $\Delta G^{\ddagger}_{re}$ values ∼5 kcal mol^{-1} higher than those with one ortho fluorine. The stabilities of complexes with two ortho fluorines seemed to be less influenced by additional fluorine substituents, while complexes with one ortho fluorine seemed to be slightly more affected by additional fluorines. The free energy difference between the Tp′Rh(CNneopentyl)(aryl$_F$)H products was used to calculate M−C bond strengths relative to the M−C bond strength in Tp′Rh(CNneopentyl)(C_6F_5)H. The M−C bond strengths changed by ∼13 kcal mol^{-1}, while the analogous calculated C−H bond strengths spanned ∼6 kcal mol^{-1}. Plotting the experimentally determined ΔD(Rh−C) vs D(C−H) gives a slope of 2.14, much larger than previous M−C/H−C bond energy correlations on unsubstituted aliphatics and aromatics. A similar plot using calculated D(Rh−C) values gives a very similar distribution of data and a slope of 2.0. The electron-withdrawing effect of the ortho fluorine greatly strengthens the M−C bond by ∼7 kcal mol^{-1}.

Experimental Section

General Procedures. All operations and routine manipulations were performed under a nitrogen atmosphere, either on a high-vacuum line using modified Schlenk techniques or in a Vacuum Atmospheres Corp. Dri-Lab. Benzene-d_6 was distilled under vacuum from a dark purple solution of benzophenone ketyl and stored in an ampule with a Teflon valve. Fluorinated aromatic compounds were purchased from Aldrich Chemical Co. and TCI America, dried over magnesium sulfate, and vacuum-distilled prior to use. Preparation of Tp′Rh(CNneopentyl)(η^2-PhN═C═N-neopentyl) (**1**) has been previously reported.[38]

All ^{1}H NMR and ^{19}F NMR spectra were recorded on a Bruker Avance 400 MHz NMR spectrometer. All ^{1}H chemical shifts are reported in ppm (δ) relative to tetramethylsilane and referenced to the chemical shift of residual solvent (benzene, δ 7.16). ^{19}F NMR spectra were referenced to external $C_6H_5CF_3$ (δ 0). All temperatures for variable-temperature NMR spectroscopy were calibrated relative to the chemical shift differences in the NMR spectra of known standards (25−80 °C, ethylene glycol). All photolysis experiments were carried out using a water-filtered 200-W Hg−Xe lamp.

Computational Details. All calculations were performed with the Gaussian03 package[41] of programs with the hybrid B3PW91 functional.[42,43] The Rh atom was represented by the relativistic effective core potential (RECP) from the Stuttgart group and the associated basis set,[44] augmented by an f polarization function.[45] The remaining atoms (C, H, N, B, F) were represented by a 6-31G(d,p) basis set.[46] Full optimization of geometry was performed without any constraint, followed by analytical computation of the Hessian matrix to identify the nature of the located extrema as minima. ^{19}F shielding constants were calculated to assist in the experimental assignments. See Supporting Information for details.

Preparation of Tp′Rh(CNneopentyl)(C_6F_5)H (2). A solution of **1** (9 mg, 0.013 mmol) dissolved in 0.5 mL of pentafluorobenzene was placed in an NMR tube sealed with a Teflon cap. This sample was irradiated for 30 min at −20 °C. The solvent was immediately removed *in vacuo* at room temperature. The resulting yellow residue was dissolved in C_6D_6, and ^{1}H and ^{19}F NMR spectra were collected. ^{1}H NMR (C_6D_6): δ −13.174 (t, $J_{Rh-H} = J_{F-H} =$ 17.4 Hz, 1 H), 0.566 (s, 9 H, C(CH$_3$)$_3$), 1.661 (s, 3 H, pz CH$_3$), 1.997 (s, 3 H, pz CH$_3$), 2.135 (s, 3 H, pz CH$_3$), 2.166 (s, 3 H, pz CH$_3$), 2.308 (s, 3 H, pz CH$_3$), 2.393 (s, 3 H, pz CH$_3$), 2.498 (ABq, $J_{Rh-H} =$ 24.3, 14.0 Hz, 2 H, NCH$_2$), 5.486 (s, 1 H, pz H), 5.645 (s, 1 H, pz H), 5.823 (s, 1 H, pz H). ^{19}F NMR (C_6D_6): δ −43.47 (m, 1 F$_{ortho}$), −57.86 (m, 1 F$_{ortho}$), −101.48 (t, 1 F$_{para}$), −103.27 (m, 1 F$_{meta}$), −103.59 (m, 1 F$_{meta}$). ^{1}H{^{19}F} NMR (C_6D_6): δ −13.174 (d, $J_{Rh-H} =$ 17.4 Hz, 1 H), other resonances unchanged.

Preparation of Tp′Rh(CNneopentyl)(2,3,5,6-C_6F_4H)H (3). A solution of **1** (9 mg, 0.013 mmol) dissolved in 0.5 mL of 1,2,4,5-tetrafluorobenzene was placed in an NMR tube sealed with a Teflon cap. This sample was irradiated for 30 min at 10 °C. The solvent was immediately removed *in vacuo* at room temperature. The resulting yellow residue was dissolved in C_6D_6, and ^{1}H and ^{19}F NMR spectra were collected. ^{1}H NMR (C_6D_6): δ −13.095 (t, $J_{Rh-H} = J_{F-H} =$ 17.3 Hz, 1 H), 0.572 (s, 9 H, C(CH$_3$)$_3$), 1.725 (s, 3 H, pz CH$_3$), 2.047 (s, 3 H, pz CH$_3$), 2.139 (s, 3 H, pz CH$_3$), 2.177 (s, 3 H, pz CH$_3$), 2.316 (s, 3 H, pz CH$_3$), 2.425 (s, 3 H, pz CH$_3$), 2.501 (ABq, $J =$ 23.3, 13.7 Hz, 2 H, NCH$_2$), 5.470 (s, 1 H, pz H), 5.656 (s, 1 H, pz H), 5.829 (s, 1 H, pz H), 6.932 (t, 1 H, aryl$_F$ H). ^{19}F NMR (C_6D_6): δ −44.78 (m, 1 F$_{ortho}$), −59.49 (m, 1 F$_{ortho}$), −79.16 (m, 1 F$_{meta}$), −80.12 (m, 1 F$_{meta}$). ^{1}H{^{19}F} NMR (C_6D_6): δ −13.095 (d, $J_{Rh-H} =$ 17.3 Hz, 1 H), other resonances unchanged.

Preparation of Tp′Rh(CNneopentyl)(2,4,6-$C_6F_3H_2$)H (4). The synthesis of **4** was identical to that of **3** except that **1** was dissolved in 0.5 mL of 1,3,5-trifluorobenzene. ^{1}H NMR (C_6D_6): δ −13.233 (dd, $J_{Rh-H} =$ 18.9 Hz, $J_{F-H} =$ 14.8 Hz, 1 H), 0.619 (s, 9 H, C(CH$_3$)$_3$), 1.801 (s, 3 H, pz CH$_3$), 2.127 (s, 3 H, pz CH$_3$), 2.167 (s, 3 H, pz CH$_3$), 2.199 (s, 3 H, pz CH$_3$), 2.333 (s, 3 H, pz CH$_3$), 2.451 (s, 3 H, pz CH$_3$), 2.565 (ABq, $J =$ 23.9, 13.7 Hz, 2 H, NCH$_2$), 5.516 (s, 1 H, pz H), 5.674 (s, 1 H, pz H), 5.863 (s, 1 H, pz H), 6.326 (t, 1 H, aryl$_F$ H), 6.706 (t, 1 H, aryl$_F$ H). ^{19}F NMR (C_6D_6): δ −11.83 (m, 1 F$_{ortho}$), −24.60 (m, 1 F$_{ortho}$), −57.11 (m, 1 F$_{para}$). ^{1}H−^{19}F HETCOR (C_6D_6): see Supporting Information.

Preparation of Tp′Rh(CNneopentyl)(2,5-$C_6F_2H_3$)H (5). The synthesis of **5** was identical to that of **2** except that **1** was dissolved in 0.5 mL of *p*-difluorobenzene. ^{1}H NMR (C_6D_6): δ −13.384 (dd, $J_{Rh-H} =$ 21.5 Hz, $J_{F-H} =$ 12.9 Hz, 1 H), 0.634 (s, 9 H, C(CH$_3$)$_3$), 1.770 (s, 3 H, pz CH$_3$), 2.074 (s, 3 H, pz CH$_3$), 2.128 (s, 3 H, pz CH$_3$), 2.205 (s, 3 H, pz CH$_3$), 2.298 (s, 3 H, pz CH$_3$), 2.441 (s, 3 H, pz CH$_3$), 2.603 (ABq, $J =$ 19.7, 14.0 Hz, 2 H, NCH$_2$), 5.465 (s, 1 H, pz H), 5.668 (s, 1 H, pz H), 5.812 (s, 1 H, pz H), 6.609 (m, 1 H, aryl$_F$ H), 6.867 (m (overlaps with free carbodiimide), 1 H, aryl$_F$ H), 6.973 (m, 1 H, 6.937). ^{19}F NMR (C_6D_6): δ −29.35 (m, 1 F$_{ortho}$), −60.44 (m, 1 F$_{meta}$).

Preparation of Tp′Rh(CNneopentyl)(2,3,4,5-C_6F_4H)H (6). The synthesis of **6** was identical that of **2** except that **1** was dissolved in 0.5 mL of 1,2,3,4-tetrafluorobenzene. ^{1}H NMR (C_6D_6): δ −13.40 (dd, $J_{Rh-H} =$ 20.5 Hz, $J_{F-H} =$ 14.7 Hz, 1 H), 0.580 (s, 9 H, C(CH$_3$)$_3$), 1.962 (s, 3 H, pz CH$_3$), 2.111 (s, 3 H, pz CH$_3$), 2.175 (s, 3 H, pz CH$_3$), 2.277 (s, 3 H, pz CH$_3$), 2.386 (s, 3 H, pz CH$_3$), 2.760 (s, 3 H, pz CH$_3$), 2.524 (ABq, $J =$ 26.3, 20.4 Hz, 2 H, NCH$_2$), 5.449 (s, 1 H, pz H), 5.646 (s, 1 H, pz H), 5.802 (s, 1 H, pz H),

(41) Frisch, M. J.; et al. *Gaussian 03*, Revision C.02; Gaussian Inc.: Wallingford, CT, 2004.
(42) Becke, A. D. *J. Chem. Phys.* **1993**, *98*, 5648.
(43) Perdew, J. P.; Wang, Y. *Phys. Rev. B* **1992**, *45*, 13244.
(44) Andrae, D.; Häussermann, U.; Dolg, M.; Stoll, H.; Preuss, H. *Theor. Chim. Acta* **1990**, *77*, 123.
(45) Ehlers, A. W.; Böhme, M.; Dapprich, S.; Gobbi, A.; Höllwarth, A.; Jonas, V.; Köhler, K. F.; Stegmann, R.; Veldkamp, A.; Frenking, G. *Chem. Phys. Lett.* **1993**, *208*, 111.
(46) Hariharan, P. C.; Pople, J. A. *Theor. Chim. Acta* **1973**, *28*, 213.

6.552 (m, 1 H, $aryl_F$). ^{19}F NMR (C_6D_6): δ −48.88 (m, 1 F_{ortho}), −81.00 (m, 1 F_{meta}), −97.71 (m, 1 F_{meta}), −103.24 (m, 1 F_{para}).

Preparation of Tp′Rh(CNneopentyl)(3,4-$C_6H_3F_2$)H (7a) and Tp′Rh(CNneopentyl)(2,3-$C_6H_3F_2$)H (7b). The syntheses of **7a** and **7b** were identical to that of **2** except that **1** was dissolved in 0.5 mL of *o*-difluorobenzene. It was determined by ^{19}F NMR that photolysis resulted in two major products, **7a** and **7b**, in a ratio of 1.5:1. ^1H NMR (C_6D_6) for **7a**: δ −13.76 (d, J_{Rh-H} = 23.5 Hz, 1 H). ^{19}F NMR (C_6D_6) for **7a**: δ −81.10 (m, 1 F_{para}), −86.96 (m, 1 F_{meta}). The products of photolysis were then heated to 100 °C for 10 days in neat *o*-difluorobenzene, resulting in complete conversion of **7a** to **7b**. Integration of the sum of the hydride resonances relative to the sum of the Tp′ resonances showed ∼87% yield of **7b**. ^1H NMR (C_6D_6) for **7a**: δ −13.758 (d, J_{Rh-H} = 25.3 Hz), 0.579 (s, 9 H, $C(CH_3)_3$), 1.819 (s, 3 H, pz CH_3), 2.000 (s, 3 H, pz CH_3), 2.168 (s, 3 H, pz CH_3), 2.222 (s, 3 H, pz CH_3), 2.374 (s, 3 H, pz CH_3), 2.761 (s, 3 H, pz CH_3), 5.528 (s, 1 H, pz H), 5.679 (s, 1 H, pz H), 5.863 (s, 1 H, pz H). ^1H NMR (C_6D_6) for **7b**: δ −13.392 (dd, J_{Rh-H} = 21.3 Hz, J_{F-H} = 14.1 Hz), 0.610 (s, 9 H, $C(CH_3)_3$), 1.709 (s, 3 H, pz CH_3), 2.050 (s, 3 H, pz CH_3), 2.167 (s, 3 H, pz CH_3), 2.215 (s, 3 H, pz CH_3), 2.335 (s, 3 H, pz CH_3), 2.456 (s, 3 H, pz CH_3), 2.539 (AB_q, J = 35.7 Hz, 2 H, NCH_2), 5.479 (s, 1 H, pz H), 5.678 (s, 1 H, pz H), 5.846 (s, 1 H, pz H), 6.803 (m, 2 H, $aryl_F$), ∼7.3 (m, 1 H). ^{19}F NMR (C_6D_6): δ −48.26 (m, 1 F_{ortho}), −78.34 (m, 1 F_{meta}). ^1H NMR also showed the presence of three C−H activation products, corresponding to ortho, meta, and para C−H bond activation of the carbodiimide ligand, that have been characterized previously.[38] These products were no longer observable in the NMR spectrum after thermolysis in neat *o*-difluorobenzene at 100 °C for 10 days. ^1H NMR (C_6D_6) for these minor products: δ −13.391 (d, J_{Rh-H} = 22.5 Hz, 1 H), −13.658 (d, J_{Rh-H} = 24 Hz), −13.676 (d, J_{Rh-H} = 24 Hz, 1 H).

Preparation of Tp′Rh(CNneopentyl)(2,4-$C_6H_3F_2$)H (8a), Tp′Rh(CNneopentyl)(3,5-$C_6H_3F_2$)H (8b), and Tp′Rh(CNneopentyl)(2,6-$C_6H_3F_2$)H (8c). Preparations of **8a**, **8b**, and **8c** were identical to that of **2** except that **1** was irradiated in 0.5 mL of *m*-difluorobenzene. It was determined by ^{19}F NMR that photolysis resulted in three major products, **8a**, **8b**, and **8c**, in a ratio of 10:4:1. ^1H NMR (C_6D_6) for **8a**: δ −13.485 (dd, J_{Rh-H} = 21.5 Hz, J_{F-H} = 13.1 Hz, 1 H). ^{19}F NMR (C_6D_6) for **8a**: δ −19.62 (m, 1 F_{ortho}), −59.1 (m, 1 F_{para}). ^1H NMR (C_6D_6) for **8b**: δ −13.629 (d, J_{Rh-H} = 23.6 Hz, 1 H). ^{19}F NMR (C_6D_6) for **8b**: δ −52.06 (m, 1 F_{meta}), −54.23 (m, 1 F_{meta}). Heating **8a**, **8b**, and **8c** to 100 °C for 30 days in neat *m*-difluorobenzene did not result in complete conversion of **8a** and **8b** to **8c**, as decomposition of the sample was observed. Integration of the sum of the hydride resonances relative to the sum of the Tp′ resonances showed ∼67% yield of **8c**. ^1H NMR (C_6D_6) for **8c**: δ −13.154 (dd, J_{Rh-H} = 19.7 Hz, J_{F-H} = 14.7 Hz, 1 H). ^{19}F NMR (C_6D_6) for **8c**: δ −14.06 (m, 1 F_{ortho}), −27.68 (m, 1 F_{ortho}). ^1H NMR also showed the presence of three C−H activation products, corresponding to ortho, meta, and para C−H bond activation of the phenyl ring of the released carbodiimide ligand. After thermolysis in neat *m*-difluorobenzene for 10 days at 100 °C, these minor products were no longer observed by NMR spectroscopy.

Preparation of Tp′Rh(CNneopentyl)(3-C_6H_4F)H (9b), Tp′Rh(CNneopentyl)(4-C_6H_4F)H (9a), and Tp′Rh(CNneopentyl)(2-C_6H_4F)H (9c). Preparations of **9a**, **9b**, and **9c** were identical to that of **2** except that **1** was irradiated in 0.5 mL of fluorobenzene. It was determined by ^{19}F NMR that photolysis resulted in three major products, **9a**, **9b**, and **9c**, in a ratio of 1:2:2. ^1H NMR (C_6D_6) for **9a**: δ −13.67 (br d, J_{Rh-H} = 24 Hz). ^{19}F NMR (C_6D_6): δ −55.35 (m, 1 F_{para}). ^1H NMR (C_6D_6) for **9b**: δ −13.738 (d, J_{Rh-H} = 24.2 Hz, 1 H). ^{19}F NMR (C_6D_6): δ −61.81 (m, 1 F_{meta}). The products of photolysis were then heated to 100 °C for 10 days in neat fluorobenzene, resulting in conversion of products **9a** and **9b** to only **9c**. Integration of the sum of the hydride resonances relative to the sum of the Tp′ resonances showed ∼79% yield of **9c**. ^1H NMR (C_6D_6) for **9c**: ^1H NMR (C_6D_6): δ −13.417 (dd, J_{Rh-H} = 22.0 Hz, J_{F-H} = 13.0 Hz, 1 H), 0.652 (s, 9 H, $C(CH_3)_3$), 1.761 (s, 3 H, pz CH_3), 2.098 (s, 3 H, pz CH_3), 2.185 (s, 3 H, pz CH_3), 2.236 (s, 3 H, pz CH_3), 2.353 (s, 3 H, pz CH_3), 2.483 (s, 3 H, pz CH_3), 2.601 (ABq, J = 17.8, 14.3 Hz, 2 H, NCH_2), 5.495 (s, 1 H, pz H), 5.693 (s, 1 H, pz H), 5.857 (s, 1 H, pz H). ^{19}F NMR (C_6D_6): δ −22.12 (m, 1 F_{ortho}). ^1H NMR also showed the presence of three C−H activation products, corresponding to ortho, meta, and para C−H bond activation of the carbodiimide ligand, which disappeared upon heating to 100 °C.

Preparation of Tp′Rh(CNneopentyl)(C_6F_5)Cl (2-Cl). A solution of Tp′Rh(CNneopentyl)(η^2-PhN=C=N-neopentyl) (9 mg, 0.013 mmol) in 0.5 mL of pentafluorobenzene was irradiated in an NMR tube as described previously. Volatiles were then removed under vacuum, leaving a pale-yellow residue which was dissolved in hexane. This solution was added to 1 mL of carbon tetrachloride under inert conditions at −20 °C. The mixture was maintained at −20 °C for 3 h, after which point the solvent was removed *in vacuo*. The crude product was crystallized from slow evaporation of CH_2Cl_2:hexane at room temperature. ^1H NMR (C_6D_6): δ 0.576 (s, 9 H, $C(CH_3)_3$), 1.600 (s, 3 H, pz CH_3), 2.064 (s, 3 H, pz CH_3), 2.135 (s, 3 H, pz CH_3), 2.145 (s, 3 H, pz CH_3), 2.201 (s, 3 H, pz CH_3), 2.849 (s, 3 H, pz CH_3), 2.589 (q, 2 H, NCH_2), 5.506 (s, 2 H, pz H), 5.666 (s, 1 H, pz H). ^{19}F NMR (C_6D_6): δ −47.41 (m, 1 F_{ortho}), −59.56 (m, 1 F_{ortho}), −98.36 (t, 1 F_{para}), −101.20 (br t, 1 F_{meta}), −101.97 (br t, 1 F_{meta}).

Solution and Refinement of Crystal Structure for Tp′Rh(CNneopentyl)(C_6F_5)Cl (2-Cl). A well-formed crystal with approximate dimensions of 0.24 × 0.08 × 0.08 mm^3 was mounted on a glass fiber and placed on a Bruker SMART APEX II CCD platform diffractometer under a cold stream of nitrogen at −173 °C. The lattice constraints were obtained from 131 reflections with values of χ between 1.54 and 29.57°. Cell reduction revealed a monoclinic crystal system. Data were collected in accord with the parameters in the Supporting Information. The space group was assigned as $P2_1/c$ on the basis of systematic absences and intensity statistics. The structure was solved using SHELXS-97. All non-hydrogen atoms were refined with anisotropic displacement parameters. The boron hydride atom was found from the difference Fourier map and refined independently from the boron atom with a relative isotropic displacement parameter. All other hydrogen atoms were placed in ideal positions and refined as riding atoms with relative isotropic displacement parameters.

Kinetics of Reductive Elimination Reactions of $aryl_F$H from Complexes 2−9. Complexes **2**−**9** were synthesized by dissolving **1** (9 mg, 0.013 mmol) in 0.5 mL of the desired fluoroarene, followed by irradiation for 30 min at the temperature shown in Table 2. Volatiles were removed *in vacuo*, resulting in a yellowish residue which was dissolved in 0.6 mL of C_6D_6, followed by 0.5 μL of hexamethyldisiloxane added as an internal standard. This solution was placed into an NMR tube, attached to a vacuum line, cooled to 78 K, and flame-sealed. The sample was warmed to room temperature and placed in a GC oven set to 138.5 °C. NMR spectra were recorded at regular intervals by ^1H NMR spectroscopy. Kinetic analysis was performed by integration of the decreasing hydride resonance relative to the signal for hexamethyldisiloxane. A first-order decay of the concentration of Tp′Rh(CNR)($aryl_F$)H was plotted against time to give the rates of reductive elimination of the corresponding $aryl_F$−H, and Excel was used to determine the rate constant. For **3** and **6**, the eliminations did not go to completion and were fit to an approach to the equilibrium

$$A \underset{k_{-1}}{\overset{k_1}{\rightleftharpoons}} B$$

using the KINSIM/FITSIM software package (see Supporting Information for kinetic data and fits).[47] Most reactions were

(47) Frieden, C. *KINSIM*; Washington University School of Medicine: St. Louis, MO, 1997; http://www.biochem.wustl.edu/cflab/message.html.

followed for 2−3 half-lives, although the elimination from **2** was so slow that it was only monitored for just over 1 half-life (37 d).

Sample Preparation and Photolysis Experiments. For entries 1−4 in Table 2, a solution of **1** (9 mg, 0.013 mmol) dissolved in 0.2 mL of pentafluorobenzene and 0.2 mL of a second arene (as indicated in Table 2) were placed in an NMR tube sealed with a Teflon cap. For entry 5, 0.05 mL of benzene and 0.4 mL of pentafluorobenzene were used. Each sample was irradiated for 30 min at the indicated temperature. The solvents were immediately removed *in vacuo* at room temperature. The resulting yellow residue was dissolved in C_6D_6, and ^{1}H and ^{19}F NMR spectra were collected. The ratio of C−H activation products was measured by integrating the fluorine resonances in the ^{19}F NMR spectrum. For entry 5, the ^{1}H hydride resonances were used to determine the product ratio. The integration ratio was used in eq 2 to calculate k_1/k_2, which was then used to calculate $\Delta\Delta G^{\ddagger}_{oa}$ according to eq 3.

Acknowledgment is made to the U.S. Department of Energy Office of Basic Energy Sciences for their support of this work (Grant FG02-86ER13569). We also thank Prof. Robin N. Perutz for helpful discussions. We acknowledge assistance from Dr. William Brennessel at the X-ray Crystallographic Facility of the Department of Chemistry at the University of Rochester.

Supporting Information Available: Tables of NMR data, kinetic data, NMR spectra, and X-ray crystallographic data for complex **2-Cl** (CCDC deposition no. 735728), coordinates and energies for calculated complexes, a summary of the calculational procedure, and complete ref 41. This material is available free of charge via the Internet at http://pubs.acs.org.

JA905057W